Supporting Information for

High Circularly Polarized Luminescence Brightness from Analogues of Shibasaki's Lanthanide Complexes

Min Deng[a], Nathan D. Schley[b], Gaël Ung*[a]

[a]Department of Chemistry, University of Connecticut, Storrs, Connecticut 06269, United States.
[b]Department of Chemistry, Vanderbilt University, Nashville, Tennessee 37235, United States.
E-mail: gael.ung@uconn.edu

Table of Contents

General Methods and Materials ····· **S2**
Synthesis of S/R-H_8-Binol Ligands ····· **S3**
General Procedure for the Synthesis of (S/R-H_8-Binol)$_3$LnNa$_3$ Complexes ····· **S3**
Synthesis of (S/R-H_8-Binol)$_3$LaNa$_3$ Complexes ····· **S3**
Synthesis of (S/R-H_8-Binol)$_3$SmNa$_3$ Complexes ····· **S4**
Synthesis of (S/R-H_8-Binol)$_3$TbNa$_3$ Complexes ····· **S4**
Synthesis of (S/R-H_8-Binol)$_3$DyNa$_3$ Complexes ····· **S4**
NMR Spectra of (S/R-H_8-Binol)$_3$LaNa$_3$ Complexes ····· **S5**
NMR Spectra of (S/R-H_8-Binol)$_3$SmNa$_3$ Complexes ····· **S7**
NMR Spectra of (S/R-H_8-Binol)$_3$TbNa$_3$ Complexes ····· **S9**
NMR Spectra of (S/R-H_8-Binol)$_3$DyNa$_3$ Complexes ····· **S10**
Absorption, Excitation and Emission Spectra of (S/R-H_8-Binol)$_3$SmNa$_3$ Complexes ····· **S11**
Absorption, Excitation and Emission Spectra of (S/R-H_8-Binol)$_3$TbNa$_3$ Complexes ····· **S12**
Absorption, Excitation and Emission Spectra of (S/R-H_8-Binol)$_3$DyNa$_3$ Complexes ····· **S13**
Emission Spectra of (S/R-H_8-Binol)$_3$EuNa$_3$ Complexes ····· **S14**
CPL g_{lum} Spectra of (S/R-H_8-Binol)$_3$SmNa$_3$ Complexes ····· **S15**
CPL g_{lum} Spectra of (S/R-H_8-Binol)$_3$TbNa$_3$ Complexes ····· **S15**
CPL g_{lum} Spectra of (S/R-H_8-Binol)$_3$DyNa$_3$ Complexes ····· **S16**
Lifetime Plot of (R-H_8-Binol)$_3$SmNa$_3$ Complex ····· **S16**
Lifetime Plot of (R-H_8-Binol)$_3$TbNa$_3$ Complex ····· **S17**
Lifetime Plot of (R-H_8-Binol)$_3$DyNa$_3$ Complex ····· **S17**
XRD Table and XRD Polyhedron Picture for (R-H_8-Binol)$_3$LaNa$_3$ ····· **S18**
CPL Brightness ····· **S19**
Reference ····· **S20**

General Methods and Material:

All operations were carried out using standard Schlenk techniques or in a Vigor glove box filled with N_2. The $Sm(OTf)_3$ was purchased from Oakwood Chemicals. The $Tb(OTf)_3$ was purchased from StremChemicals. The NaHMDS and $Dy(OTf)_3$ were purchased from Alfa Aesar. All solvents were dried using a solvent purification system from Pure Process Technology. The (R/S)-H_8-Binol were synthesized according to the literature.

NMR Spectroscopy. All NMR spectra were recorded on a Bruker AVANCE III 400 MHz spectrometer. The spectra were processed using the MestReNova software. Chemical shifts are reported in parts per million and were determined relative to the residual solvent signal (2.50 ppm for DMSO)

Photophysical Studies. All photophysical studies are performed in sealed cuvettes under dry N_2 atmosphere using anhydrous THF. Absorption, excitation, and emission spectra were recorded on a HORIBA Duetta Spectrophotometer using HORIBA EzSpec Software. Absorption spectra, excitation, and emission spectra were measured at 1.3×10^{-5} M. Circularly polarized luminescence was measured on an OLIS CPL Solo with 1.3×10^{-3} M solutions. Quantum yields were determined by absolute method using an integrating sphere on a HORIBA FLUOROMAX spectrofluorometer, all samples were measured at 4.3×10^{-6} M. Lifetimes were recorded from 1.3×10^{-4} M solutions using an OLIS CPL Solo spectrofluorometer. Spectra were collected using pulsed excitation at 340 nm and time-resolved emission measurements fixed at the peak of strongest emission. A first order exponential decay curve was fit to the collected data to estimate the fluorescence lifetime (τ_{obs}). Values are reported as measured lifetimes (observation wavelength).

XRD Studies. Single-crystal X-ray diffraction studies were performed at Vanderbilt University. A suitable crystal of each sample was selected for analysis and mounted in a polyimide loop. All measurements were made on a Rigaku Oxford Diffraction Supernova Eos CCD with filtered Mo Kα radiation at a temperature of 100 K. Using Olex2 the structure was determined with the ShelXL structure solution program using direct methods and refined with the ShelXL refinement package using least-squares minimization.

Synthesis of S-H_8-Binol Ligand

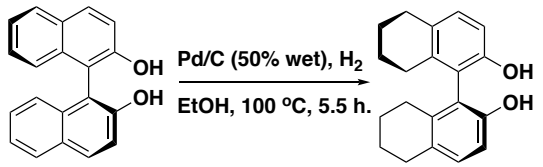

The synthesis of the S-H_8-Binol ligand followed the reported the method by using Pd/C reduction.[1] The synthesis of the R-H_8-Binol ligand is similar.

General Procedure for the Synthesis of (S-H_8-Binol)$_3$LnNa$_3$ Complexes

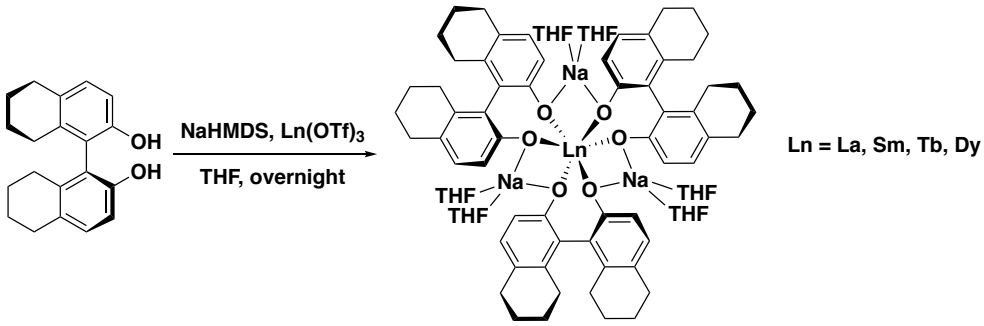

To a mixture of (S)-H_8-Binol (3.0 equiv., 0.68 mmol) and Ln(OTf)$_3$ (1 equiv., 0.23 mmol) in THF (4 mL) after stirring at room temperature for 10 minutes, a solution of NaHMDS (6 equiv., 1.36 mmol) in THF (6 mL) was added dropwise. The reaction was stirred at room temperature overnight before pumping down. The obtained solid was triturated in ACN and then centrifuged to remove the supernatant for three times. The solid residue was dissolved in THF and filtered. The filtrate was pumped down to get a solid product. The synthesis of (R-H_8-Binol)$_3$LnNa$_3$ Complexes are similar.

Synthesis of (S/R-H_8-Binol)$_3$LaNa$_3$ Complexes

(S-H_8-Binol)$_3$LaNa$_3$ was produced according to the general procedure using 133 mg of La(OTf)$_3$ (0.23 mmol) and 200 mg of S-H_8-Binol (0.68 mmol, 3.0 equiv.). Yield: 205 mg (60%) of an off-white solid. ^{1}H NMR (400 MHz, DMSO-d_6) δ 6.54 (d, J = 8.2 Hz, 6H), 6.35 (d, J = 8.1 Hz, 6H), 2.60 – 2.56 (m, 12H), 2.19 – 2.12 (m, 6H), 1.97 – 1.90 (m, 6H), 1.65 – 1.60 (m, 6H), 1.56 – 1.43 (m, 18H) ppm; ^{13}C NMR (101 MHz, DMSO-d_6) δ 161.9, 133.6, 127.7, 126.7, 119.7, 118.4, 29.1, 27.5, 23.5 (d, 2C) ppm. Elemental Analysis calc'd (%): $C_{84}H_{108}LaNa_3O_{12}$: C, 66.48; H, 7.17; found (%): C, 66.40; H, 7.12.

(R-H_8-Binol)$_3$LaNa$_3$ was produced according to the general procedure using 133 mg of La(OTf)$_3$ (0.23 mmol) and 200 mg of R-H_8-Binol (0.68 mmol, 3.0 equiv.). Yield: 204 mg (60%) of an off-white solid. ^{1}H NMR (400 MHz, DMSO-d_6) δ 6.53 (d, J = 8.2 Hz, 6H), 6.34 (d, J = 8.1 Hz, 6H), 2.59 – 2.58 (m, 12H), 2.19-2.12 (m, 6H), 1.97–1.90 (m, 6H), 1.64–1.60 (m, 6H), 1.56–1.43 (m, 18H) ppm; ^{13}C NMR (101 MHz, DMSO-d_6) δ 161.8, 133.6, 127.7, 126.7, 119.7, 118.4, 29.1, 27.5, 23.5 (d, 2C) ppm. Elemental Analysis calc'd (%): $C_{84}H_{108}LaNa_3O_{12}$: C, 66.48; H, 7.17; found (%): C, 66.42; H, 7.18.

Synthesis of (S/R-H_8-Binol)$_3$SmNa$_3$ Complexes

(S-H_8-Binol)$_3$SmNa$_3$ was produced according to the general procedure using 135 mg of Sm(OTf)$_3$ (0.23 mmol) and 200 mg of S-H_8-Binol (0.68 mmol, 3.0 equiv.). Yield: 205 mg (76%) of a white solid. ^{1}H NMR (400 MHz, DMSO-d_6) δ 5.70 (d, J = 8.0 Hz, 6H), 3.21 – 3.03 (m, 12H), 2.56 – 2.53 (m, 12H), 2.45 (s, 6H), 2.02 – 1.89 (m, 18H), 1.86 – 1.80 (m, 6H) ppm; ^{13}C NMR (101 MHz, DMSO-d_6) δ 168.56, 136.50, 131.45, 127.41, 120.33, 116.03, 30.23, 29.19, 24.72, 24.42 ppm. Elemental Analysis calc'd (%): $C_{84}H_{108}SmNa_3O_{12}$: C, 65.98; H, 7.12; found (%): C, 65.89; H, 7.10.

(R-H_8-Binol)$_3$SmNa$_3$ was produced according to the general procedure using 135 mg of Sm(OTf)$_3$ (0.23 mmol) and 200 mg of R-H_8-Binol (0.68 mmol, 3.0 equiv.). Yield: 205 mg (74%) of a white solid. ^{1}H NMR (400 MHz, DMSO-d_6) δ 5.70 (d, J = 7.9 Hz, 6H), 3.15 – 2.99 (m, 12H), 2.58 – 2.52 (m, 12H), 2.40 (s, 6H), 1.97 – 1.87 (m, 18H), 1.84 – 1.77 (m, 6H) ppm; ^{13}C NMR (101 MHz, DMSO-d_6) δ 167.8, 135.8, 130.8, 126.7, 119.6, 115.3, 29.5, 28.5, 24.0, 23.7 ppm. Elemental Analysis calc'd (%): $C_{84}H_{108}SmNa_3O_{12}$: C, 65.98; H, 7.12; found (%): C, 65.94; H, 7.08.

(Note: In proton NMR, the peak at 2.4 ppm may shift as the concentration of the sample varies.)

Synthesis of (S/R-H_8-Binol)$_3$TbNa$_3$ Complexes

(S-H_8-Binol)$_3$TbNa$_3$ was produced according to the general procedure using 137 mg of Tb(OTf)$_3$ (0.23 mmol) and 200 mg of S-H_8-Binol (0.68 mmol, 3.0 equiv.). Yield: 280 mg (81%) of a white solid. ^{1}H NMR (400 MHz, DMSO-d_6) δ 15.00 ppm, broad peaks were observed. Because of paramagnetic effects and possible dynamic processes, all peaks appear to be broad and cannot be accurately integrated. A ^{13}C NMR spectrum could not be obtained due to the paramagnetic nature of the complex. Elemental Analysis calc'd (%): $C_{84}H_{108}TbNa_3O_{12}$: C, 65.61; H, 7.08; found (%): C, 65.55; H, 7.11.

(R-H_8-Binol)$_3$TbNa$_3$ was produced according to the general procedure using 137 mg of Tb(OTf)$_3$ (0.23 mmol) and 200 mg of R-H_8-Binol (0.68 mmol, 3.0 equiv.). Yield: 260 mg (75%) of a white solid. ^{1}H NMR (400 MHz, DMSO-d_6) δ 15.00 ppm, broad peaks were observed. Because of paramagnetic effects and possible dynamic processes, all peaks appear to be broad and cannot be accurately integrated. A ^{13}C NMR spectrum could not be obtained due to the paramagnetic nature of the complex. Elemental Analysis calc'd (%): $C_{84}H_{108}TbNa_3O_{12}$: C, 65.61; H, 7.08; found (%): C, 65.56; H, 7.11.

Synthesis of (S/R-H_8-Binol)$_3$DyNa$_3$ Complexes

(S-H_8-Binol)$_3$DyNa$_3$ was produced according to the general procedure using 138 mg of Dy(OTf)$_3$ (0.23 mmol) and 200 mg of S-H_8-Binol (0.68 mmol, 3.0 equiv.). Yield: 217 mg (62%) of a white solid. ^{1}H NMR (400 MHz, DMSO-d_6) δ 21.69, 14.04, 8.09 ppm, broad peaks were observed. Because of paramagnetic effects and possible dynamic processes, all peaks appear to be broad and cannot be accurately integrated. A ^{13}C NMR spectrum could not be obtained due to the paramagnetic nature of the complex. Elemental Analysis calc'd (%): $C_{84}H_{108}DyNa_3O_{12}$-$C_4H_8O$: C, 65.51; H, 7.25; found (%): C, 65.51; H, 7.26.

(R-H_8-Binol)$_3$DyNa$_3$ was produced according to the general procedure using 138 mg of Dy(OTf)$_3$ (0.23 mmol) and 200 mg of R-H_8-Binol (0.68 mmol, 3.0 equiv.). Yield: 210 mg (60%) of a white solid. ^{1}H NMR (400 MHz, DMSO-d_6) δ 20.81, 14.14, 8.72 ppm, broad peaks were observed. Because of paramagnetic effects and possible dynamic processes, all peaks appear to be broad and cannot be accurately integrated. A ^{13}C NMR spectrum could not be obtained due to the paramagnetic nature of the complex. Elemental Analysis calc'd (%): $C_{84}H_{108}DyNa_3O_{12}$: C, 65.46; H, 7.06; found (%): C, 65.40; H, 7.04.

NMR Spectra of (S-H_8-Binol)$_3$LaNa$_3$

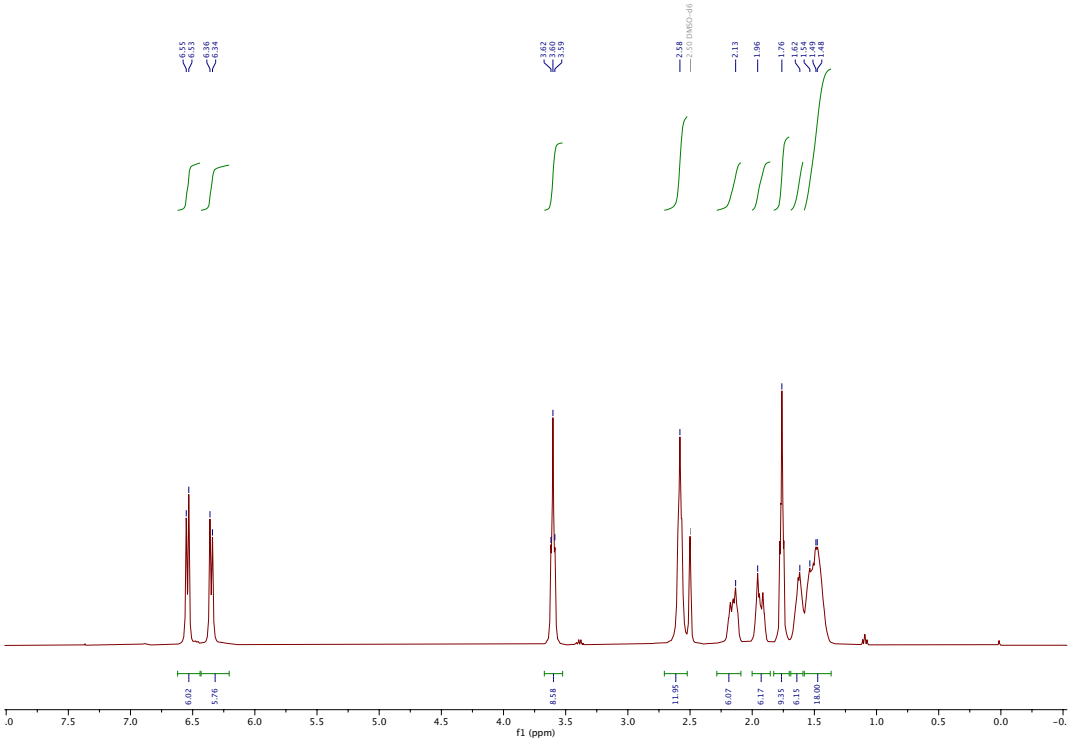

Figure S1. ^{1}H NMR of (S-H_8-Binol)$_3$LaNa$_3$ in DMSO-d_6.

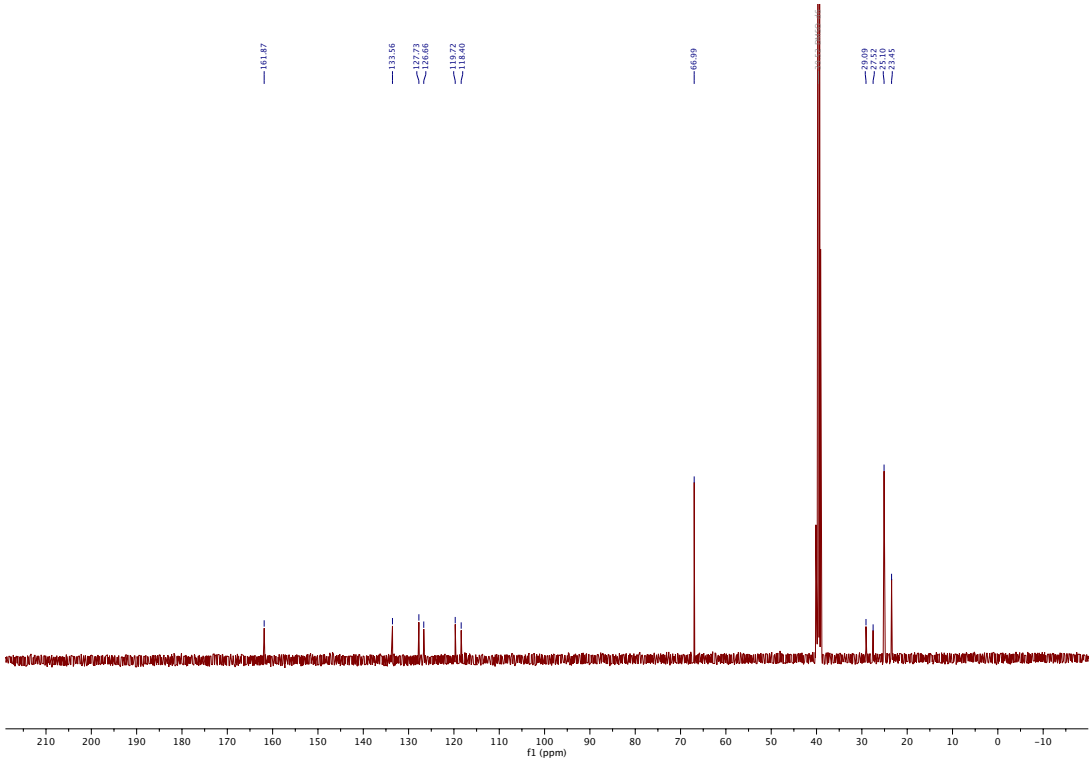

Figure S2. ^{13}C NMR of (S-H_8-Binol)$_3$LaNa$_3$ in DMSO-d_6.

NMR Spectra of (R-H_8-Binol)$_3$LaNa$_3$

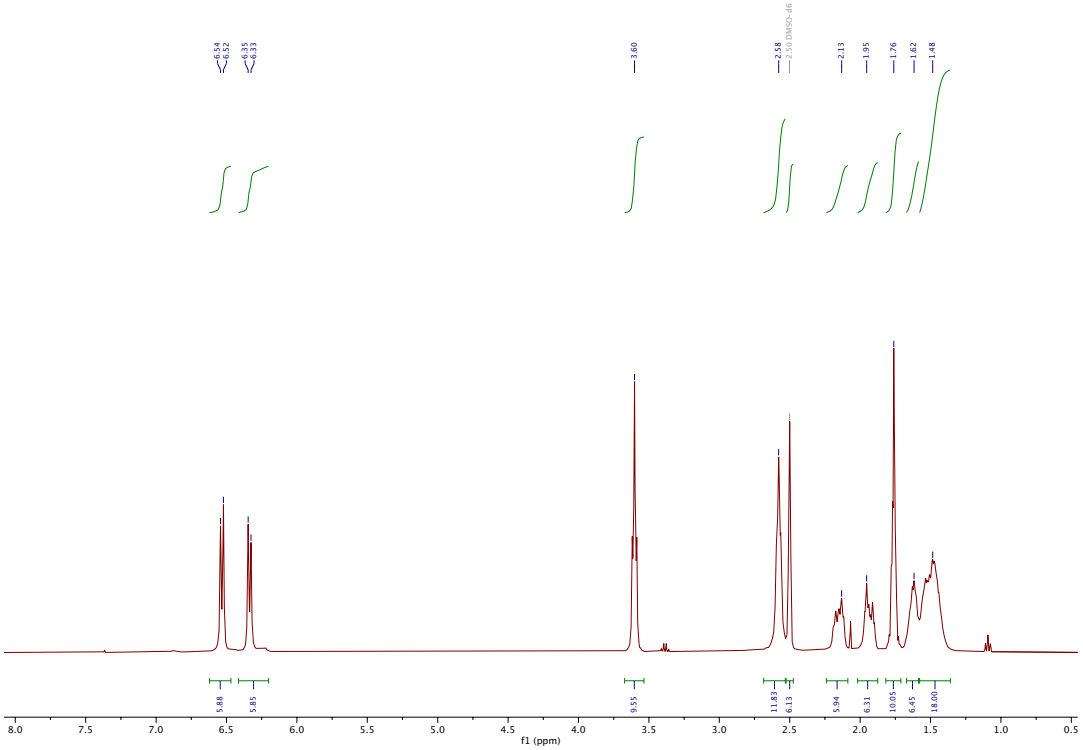

Figure S3. ^{1}H NMR of (R-H_8-Binol)$_3$LaNa$_3$ in DMSO-d_6.

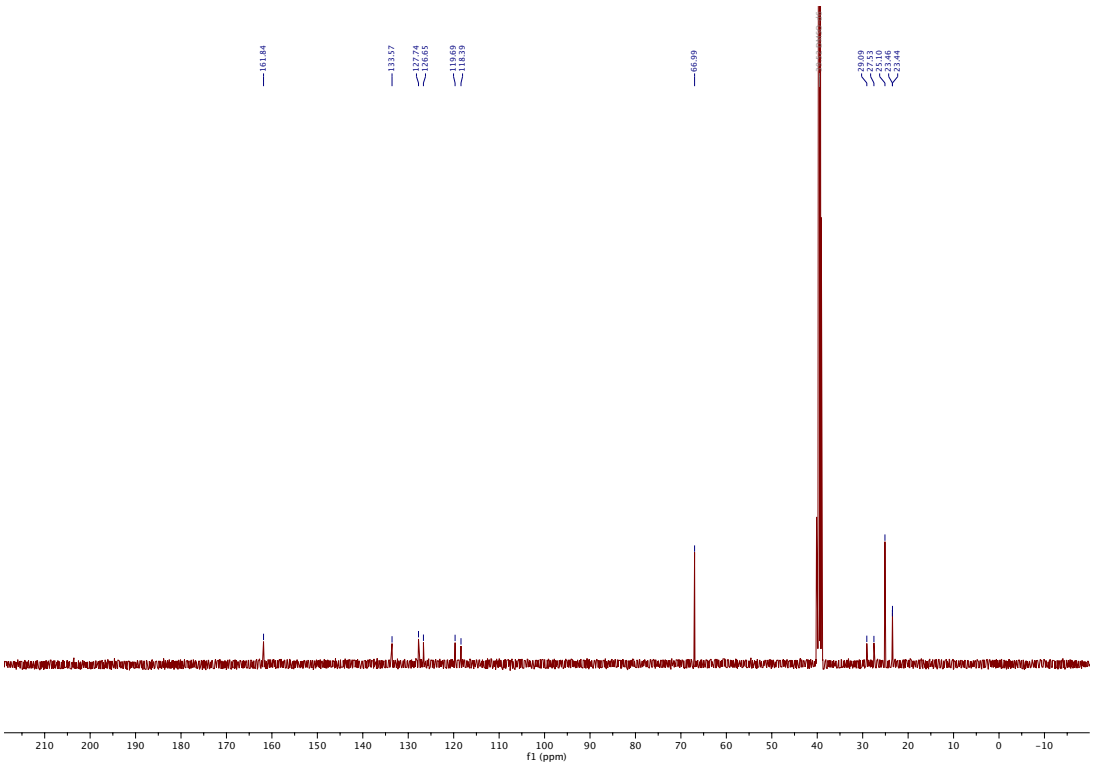

Figure S4. ^{13}C NMR of (R-H_8-Binol)$_3$LaNa$_3$ in DMSO-d_6.

NMR Spectra of (S-H_8-Binol)$_3$SmNa$_3$

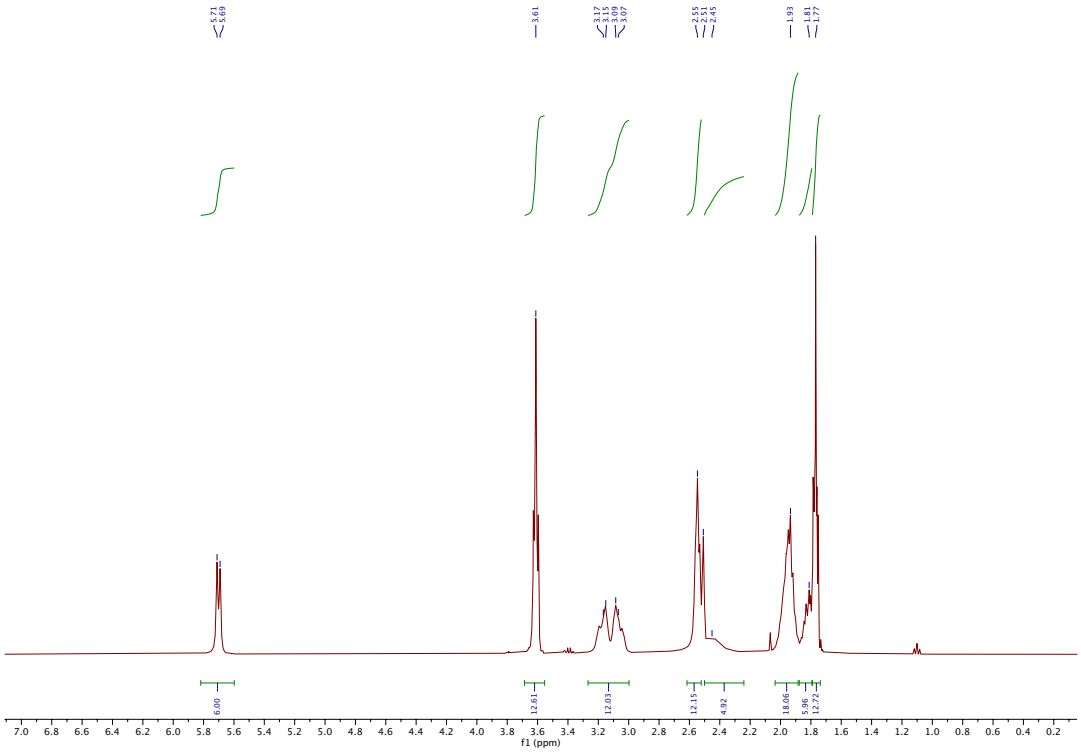

Figure S5. ^{1}H NMR of (S-H_8-Binol)$_3$SmNa$_3$ in DMSO-d_6.

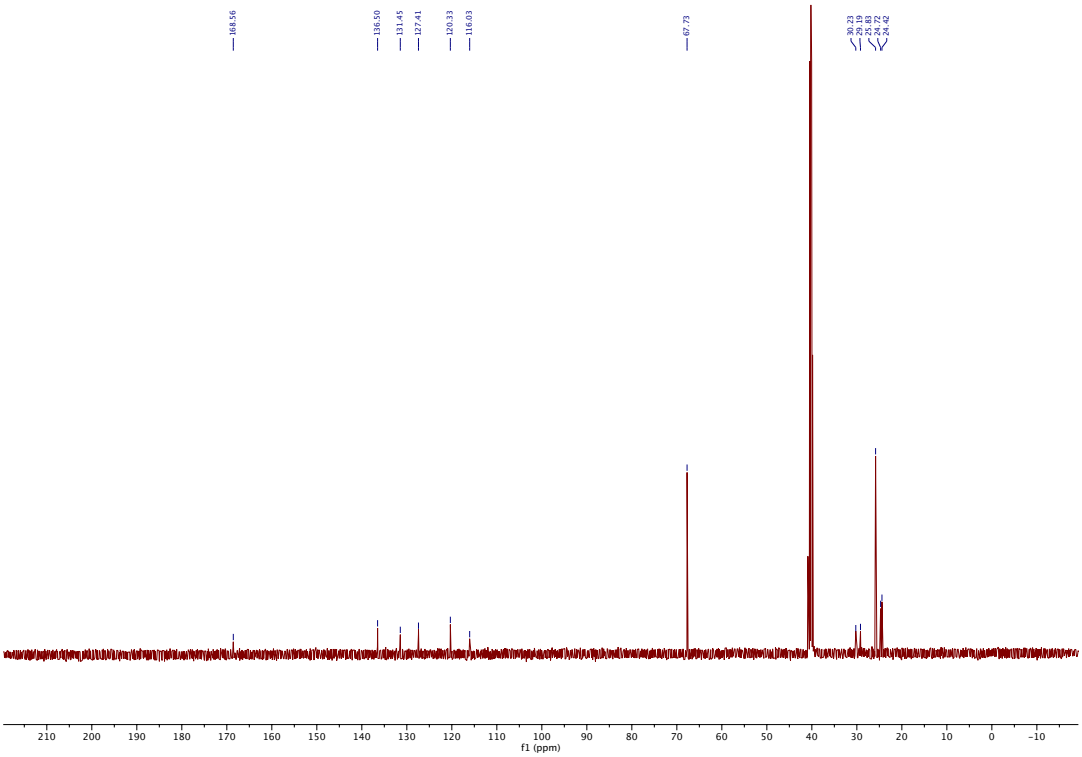

Figure S6. ^{13}C NMR of (S-H_8-Binol)$_3$SmNa$_3$ in DMSO-d_6.

NMR Spectra of (R-H_8-Binol)$_3$$SmNa_3$

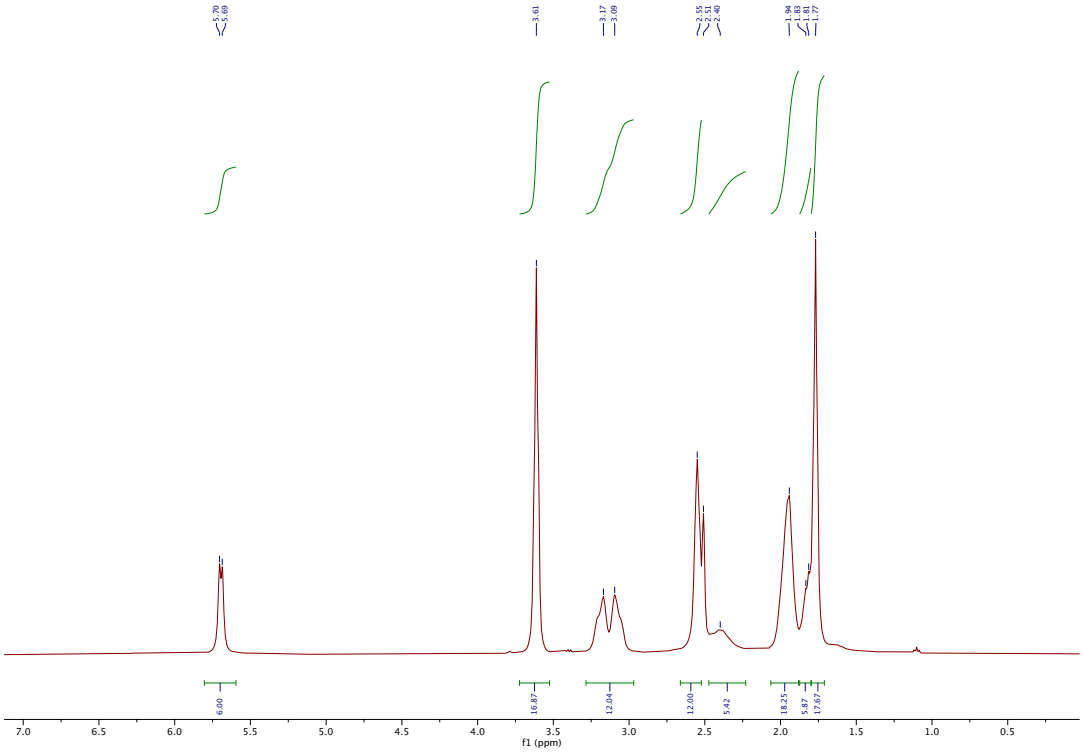

Figure S7. ^{1}H NMR of (R-H_8-Binol)$_3$$SmNa_3$ in DMSO-d_6.

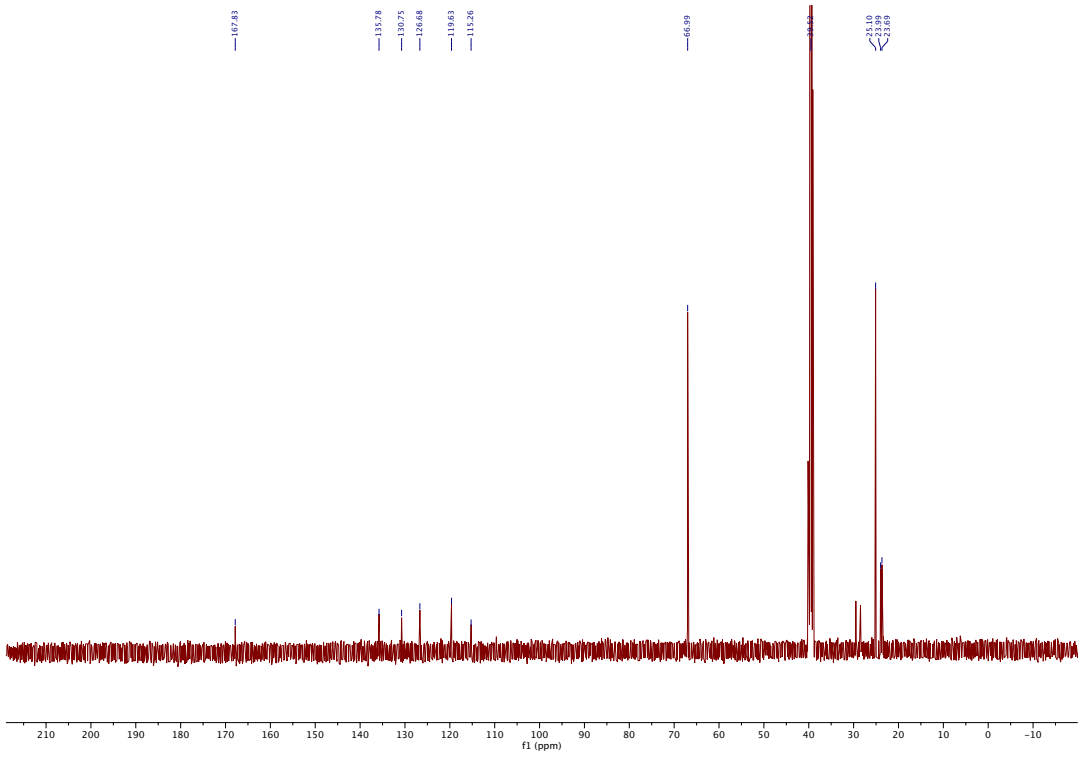

Figure S8. ^{13}C NMR of (R-H_8-Binol)$_3$$SmNa_3$ in DMSO-d_6.

NMR Spectrum (S-H_8-Binol)$_3$TbNa$_3$

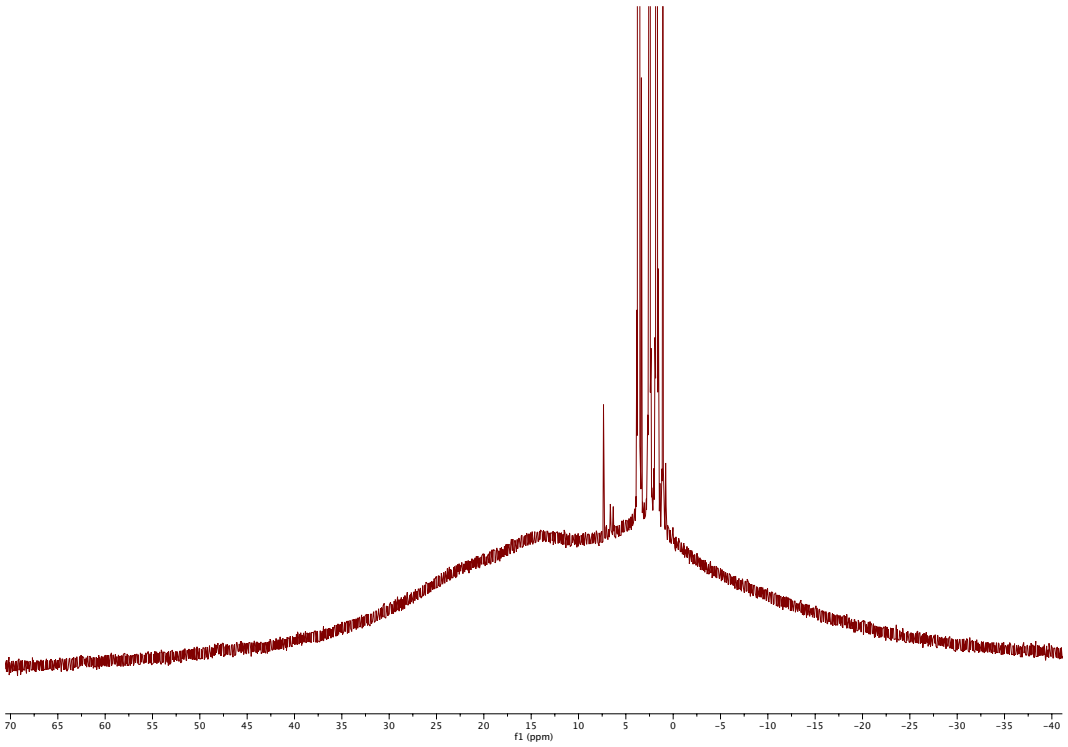

Figure S9. ^{1}H NMR of (S-H_8-Binol)$_3$TbNa$_3$ in DMSO-d_6.

NMR Spectrum of (R-H_8-Binol)$_3$TbNa$_3$

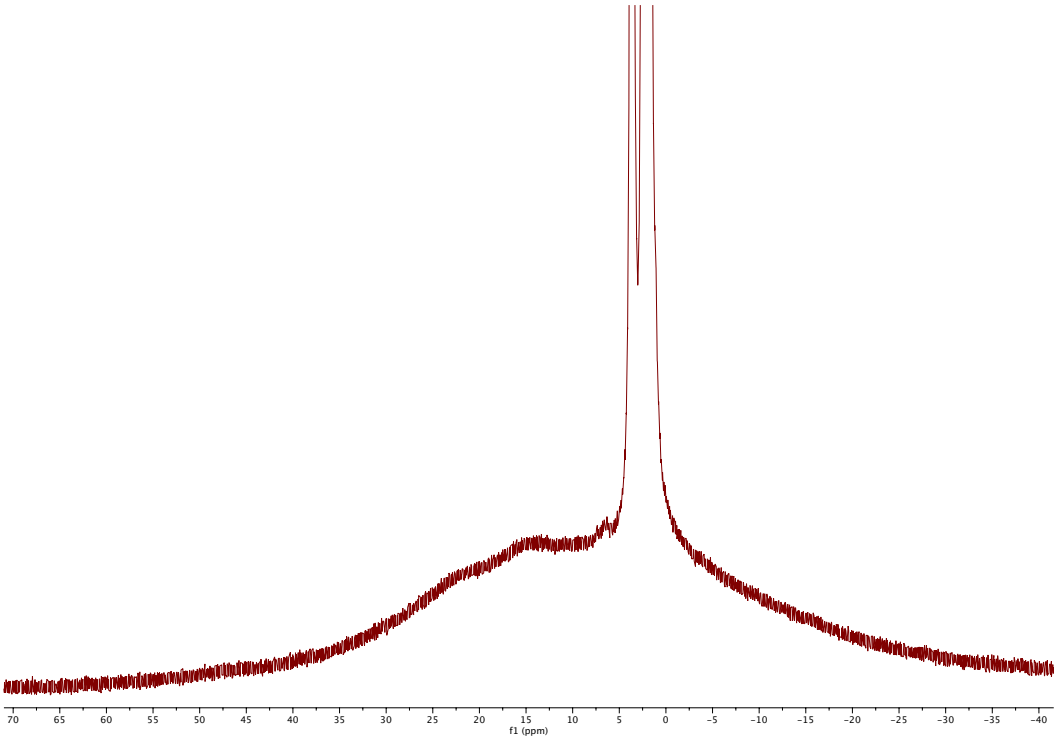

Figure S10. ^{1}H NMR of (R-H_8-Binol)$_3$TbNa$_3$ in DMSO-d_6.

NMR Spectrum of (S-H_8-Binol)$_3$DyNa$_3$

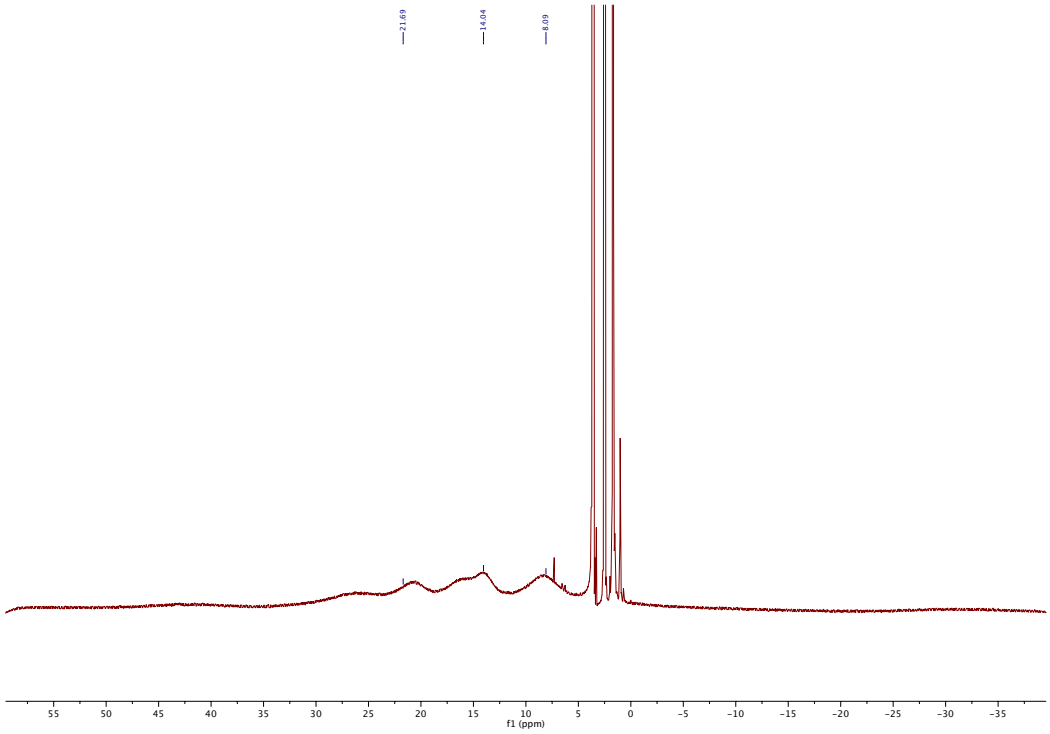

Figure S11. ^{1}H NMR of (S-H_8-Binol)$_3$DyNa$_3$ in DMSO-d_6.

NMR Spectrum of (R-H_8-Binol)$_3$DyNa$_3$

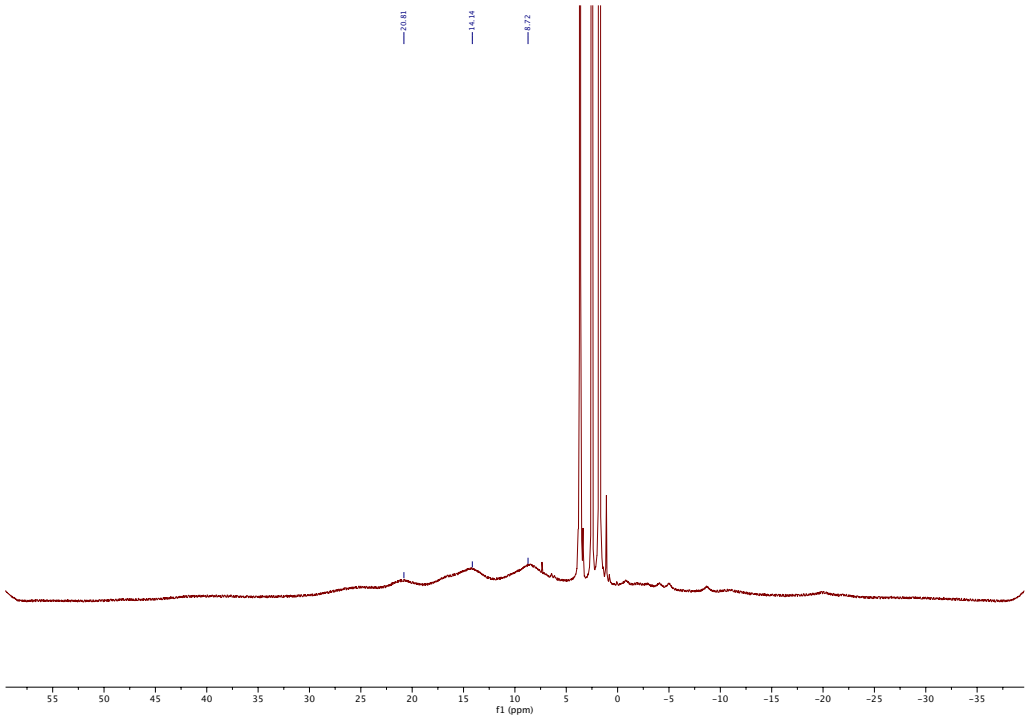

Figure S12. ^{1}H NMR of (R-H_8-Binol)$_3$DyNa$_3$ in DMSO-d_6.

Absorption, Excitation and Emission Spectra of Sm Complexes

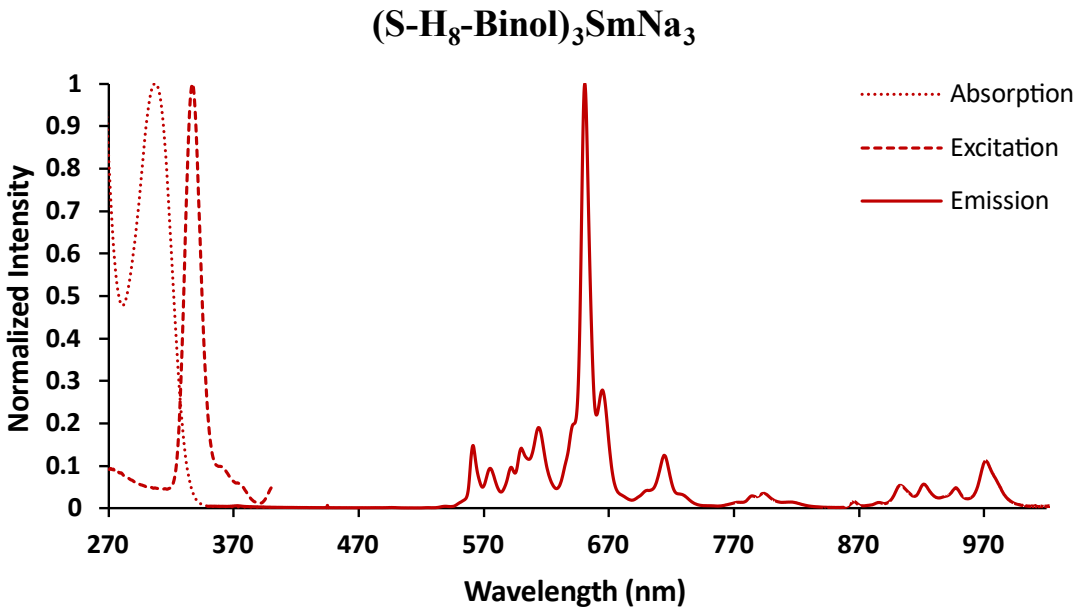

Figure S13. Normalized Absorption (dotted line), Excitation (dashed line) and Emission (solid line) spectra for (S-H_8-Binol)$_3$SmNa$_3$ complex in THF. Absorption was measured at 1.3 x 10^{-5} M, while Excitation and Emission were measured at 1.3 x 10^{-5} M. Slit widths for absorption 5 nm, for excitation 10 nm EX and EM, and for emission 5 nm EX and EM.

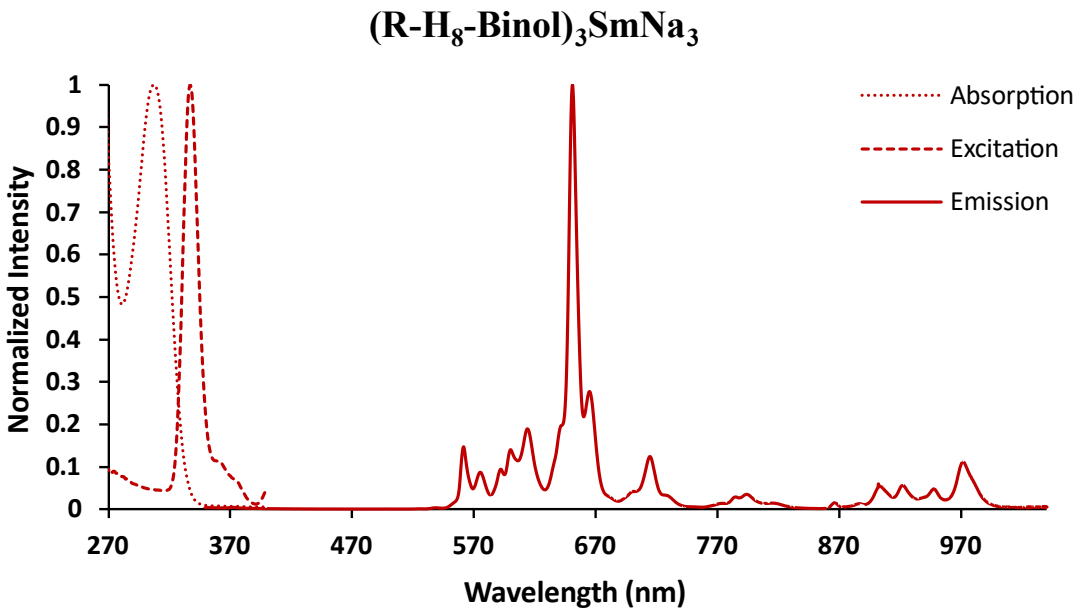

Figure S14. Normalized Absorption (dotted line), Excitation (dashed line) and Emission (solid line) spectra for (R-H_8-Binol)$_3$SmNa$_3$ complex in THF. Absorption was measured at 1.3 x 10^{-5} M, while Excitation and Emission were measured at 1.3 x 10^{-5} M. Slit widths for absorption 5 nm, for excitation 10 nm EX and EM, and for emission 5 nm EX and EM.

Absorption, Excitation and Emission Spectra of Tb Complexes

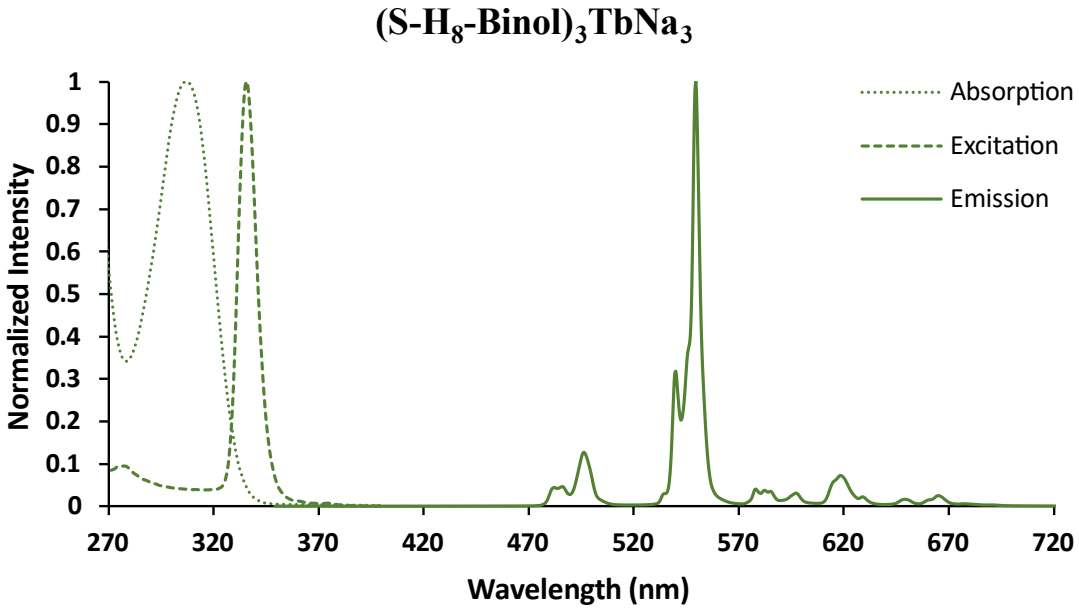

Figure S15. Normalized Absorption (dotted line), Excitation (dashed line) and Emission (solid line) spectra for (S-H_8-Binol)$_3$TbNa$_3$ complex in THF. Absorption was measured at 1.3 x 10^{-5} M, while Excitation and Emission were measured at 1.3 x 10^{-5} M. Slit widths for absorption 5 nm, for excitation 3 nm EX and EM, and for emission 2 nm EX and EM.

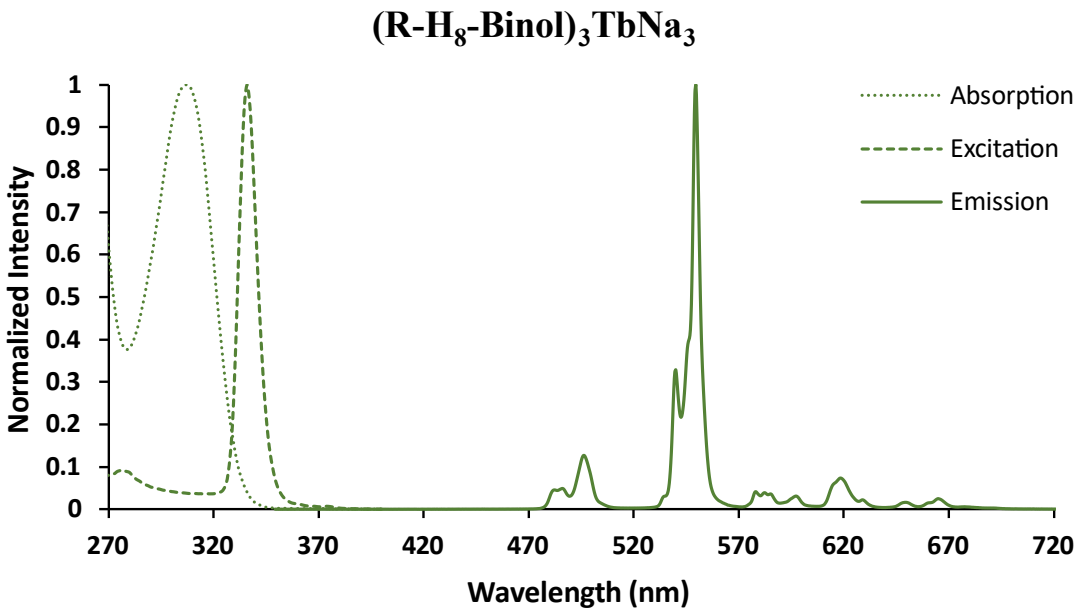

Figure S16. Normalized Absorption (dotted line), Excitation (dashed line) and Emission (solid line) spectra for (R-H_8-Binol)$_3$TbNa$_3$ complex in THF. Absorption was measured at 1.3 x 10^{-5} M, while Excitation and Emission were measured at 1.3 x 10^{-5} M. Slit widths for absorption 5 nm, for excitation 3 nm EX and EM, and for emission 2 nm EX and EM.

Absorption, Excitation and Emission Spectra of Dy Complexes

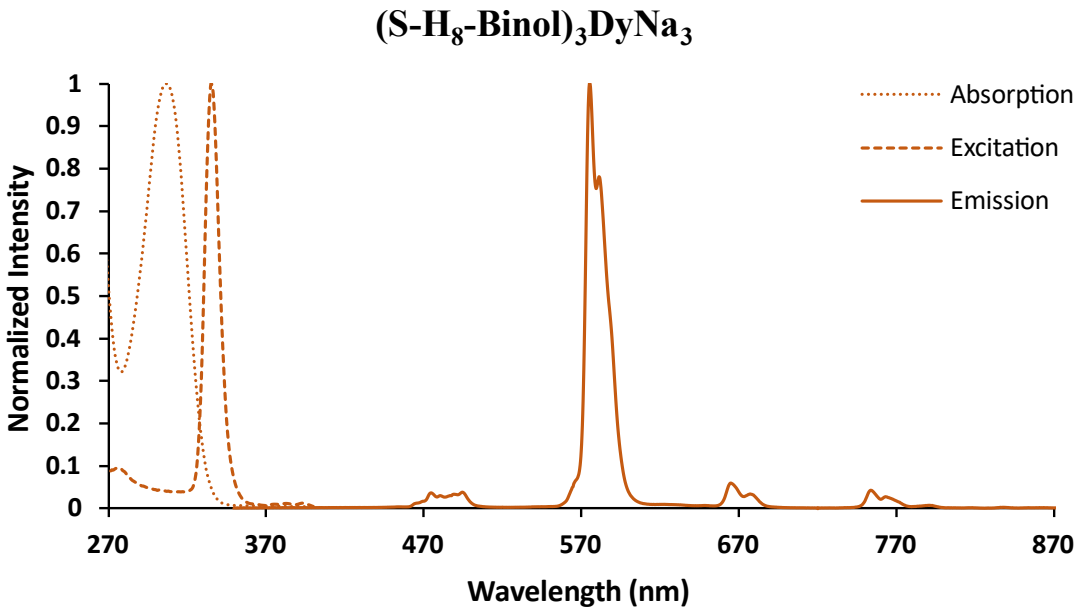

Figure S17. Normalized Absorption (dotted line), Excitation (dashed line) and Emission (solid line) spectra for (S-H_8-Binol)$_3$DyNa$_3$ complex in THF. Absorption was measured at 1.3 x 10^{-5} M, while Excitation and Emission were measured at 1.3 x 10^{-5} M. Slit widths for absorption 5 nm, for excitation 5 nm EX and EM, and for emission 3 nm EX and EM.

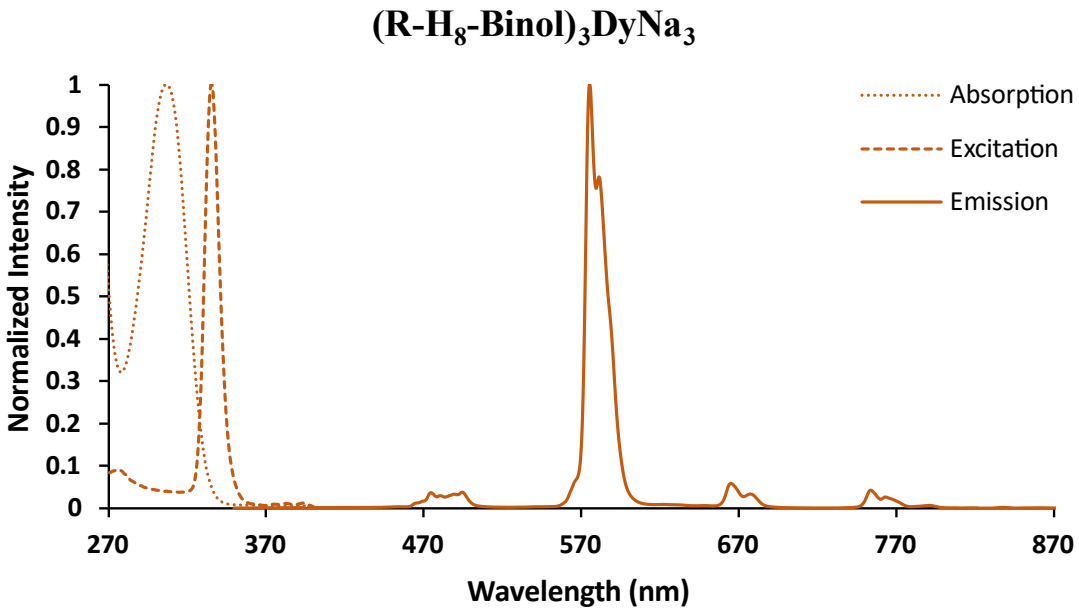

Figure S18. Normalized Absorption (dotted line), Excitation (dashed line) and Emission (solid line) spectra for (S-H_8-Binol)$_3$DyNa$_3$ complex in THF. Absorption was measured at 1.3 x 10^{-5} M, while Excitation and Emission were measured at 1.3 x 10^{-5} M. Slit widths for absorption 5 nm, for excitation 5 nm EX and EM, and for emission 3 nm EX and EM.

Note: The absorption maximum (dotted lines in Figure S13–S18) is at 310 nm, while the excitation spectra (dashed lines in Figure S13–S18) display bathochromically shifted maximum at 335 nm. These shifts and peaks similarity are reminiscent of ligand-centered sensitization of emissive lanthanide complexes reported by de Bettencourt-Dias.[2] Excitation at 335 nm gave us the best emission for $(H_8\text{-Binol})_3LnNa_3$ complexes. However, we chose to use 340 nm LED for CPL measurements because of the limitation of light sources.

Emission Spectrum of Eu Complex

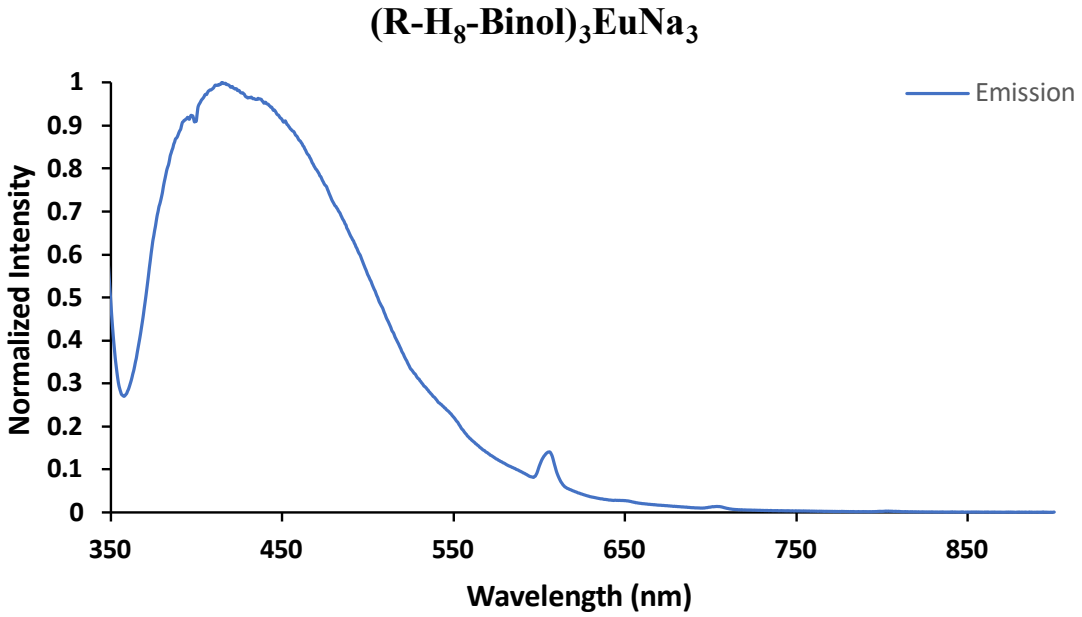

Figure S19. Normalized Emission (solid line) spectrum for $(R\text{-}H_8\text{-Binol})_3EuNa_3$ complex in THF at 1.3 x 10^{-5} M. The enantiomer $(S\text{-}H_8\text{-Binol})_3EuNa_3$ emission spectrum is identical. Slit widths: 5 nm EX and EM.

CPL g_{lum} for (S/R-H_8Binol)$_3$SmNa$_3$

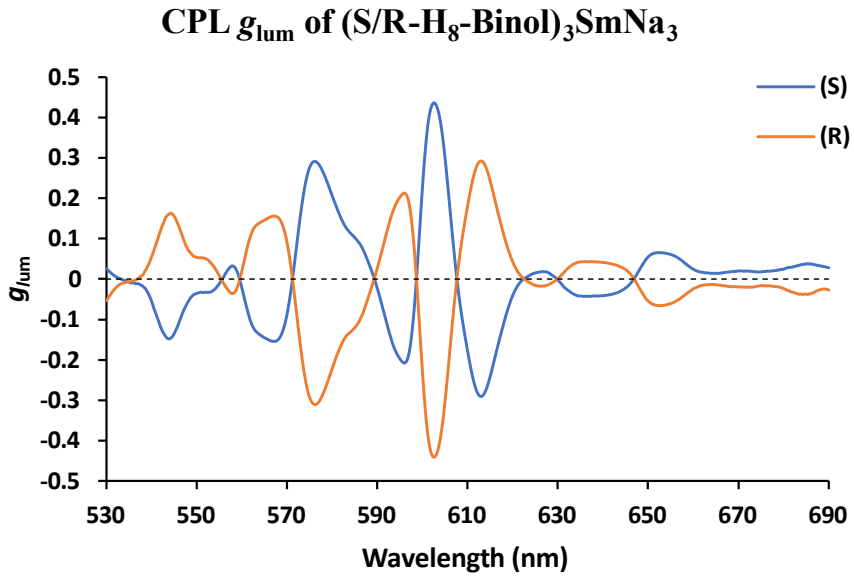

Figure S20. g_{lum} as a function of wavelength for (S/R-H_8-Binol)$_3$SmNa$_3$ complexes in THF at 1.3 x 10^{-3} M. Bandpass: 5 nm. Excitation at 340 nm. Spectra are taken as an average of 100 scans with 0.25 nm increments and 1 second integration time from 530–690 nm.

CPL g_{lum} for (S/R-H_8Binol)$_3$TbNa$_3$

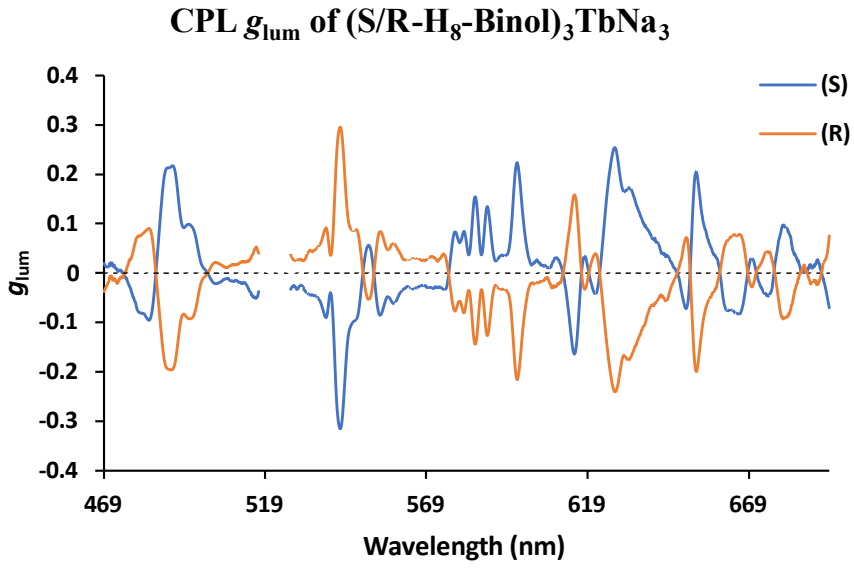

Figure S21. g_{lum} as a function of wavelength for (S/R-H_8-Binol)$_3$TbNa$_3$ complexes in THF at 1.3 x 10^{-3} M. Bandpass: 1.5 nm. Excitation at 340 nm. Spectra are taken as an average of 19 scans with 0.25 nm increments and 1 second integration time from 469–517 nm and 527–694 nm.

CPL g_{lum} for (S/R-H_8Binol)$_3$DyNa$_3$

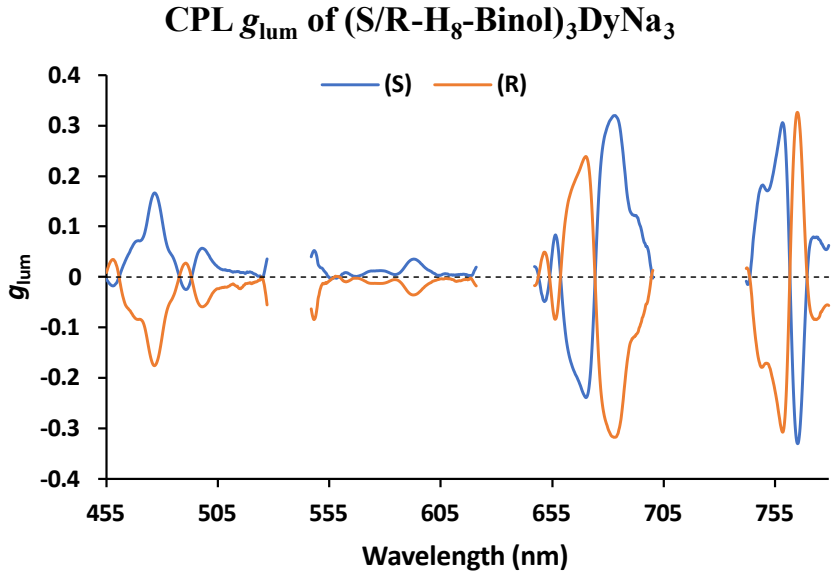

Figure S22. g_{lum} as a function of wavelength for (S/R-H_8-Binol)$_3$DyNa$_3$ complexes in THF at 1.3 x 10^{-3} M. Bandpass: 5 nm. Excitation at 340 nm. Spectra are taken as an average of 33 scans with 0.25 nm increments and 1 second integration time from 455–527 nm, 547–621 nm, 647–700 nm, and 742–779 nm.

Lifetime Plot of (R-H_8-Binol)$_3$SmNa$_3$ Complex

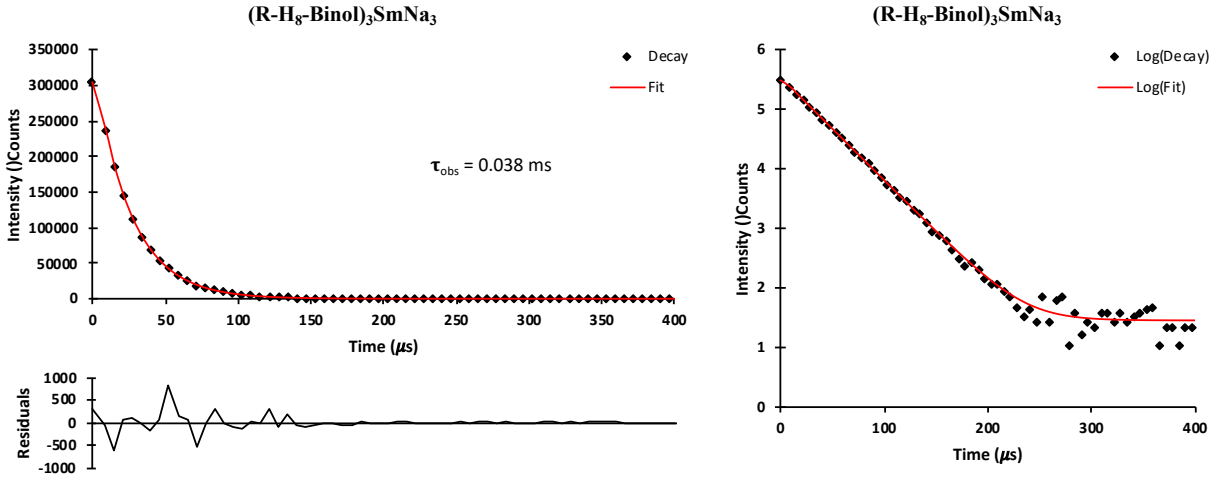

Figure S23. Lifetime exponential (left) and log (right) plots of (R-H_8-Binol)$_3$SmNa$_3$ complex for 650 nm. Excited with 340 nm LED, with a gate width of 300 (625 µs window), 200 µs delay, 200 µs LED pulse width, and 1000 events (points) taken over a 1000 µs total cycle time. Plot is an average of 30 individual runs for better resolution. The lifetime for the enantiomer is identical as expected.

Lifetime Plot of (R-H_8-Binol)$_3$TbNa$_3$ Complex

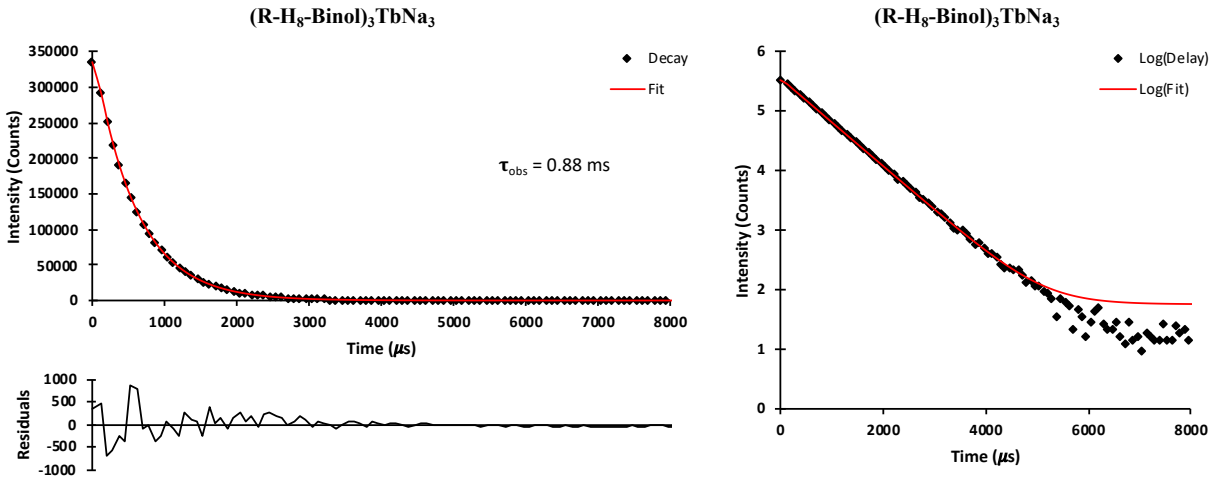

Figure S24. Lifetime exponential (left) and log (right) plots of (R-H_8-Binol)$_3$TbNa$_3$ complex for 550 nm. Excited with 340 nm LED, with a gate width of 4000 (8333 µs window), 200 µs delay, 200 µs LED pulse width, and 500 events (points) taken over a 9000 µs total cycle time. Plot is an average of 10 individual runs for better resolution. The lifetime for the enantiomer is identical as expected.

Lifetime Plot of (R-H_8-Binol)$_3$DyNa$_3$ Complex

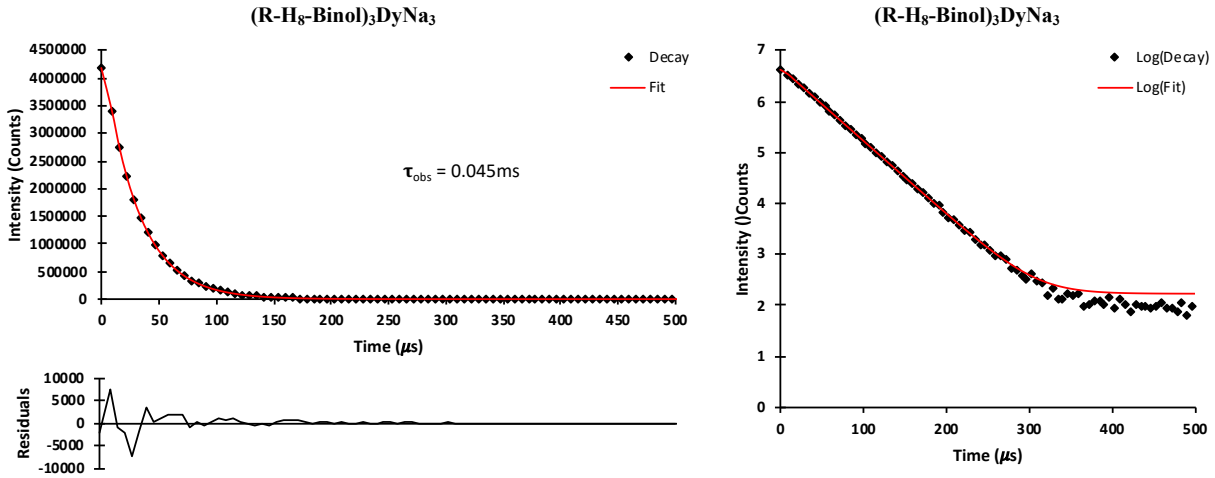

Figure S25. Lifetime exponential (left) and log (right) plots of (R-H_8-Binol)$_3$DyNa$_3$ complex for 575 nm. Excited with 340 nm LED, with a gate width of 300 (625 µs window), 500 µs delay, 500 µs LED pulse width, and 1000 events (points) taken over a 1700 µs total cycle time. Plot is an average of 30 individual runs for better resolution. The lifetime for the enantiomer is identical as expected.

XRD Table and XRD Polyhedron Picture for (R-H_8-Binol)$_3$LaNa$_3$

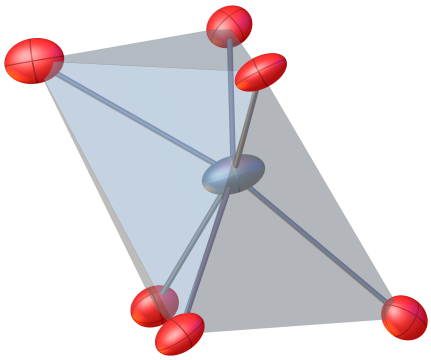

Figure S26. XRD Polyhedron Picture for (R-H_8-Binol)$_3$LaNa$_3$. Red: oxygen; Blue: lanthanum.

Table S1. Crystal data and structure refinement for (R-H_8-Binol)$_3$LaNa$_3$.

Identification code	(R-H_8-Binol)$_3$LaNa$_3$
Empirical formula	$C_{88.19}H_{116.39}LaNa_3O_{13.05}$
Formula weight	1593.14
Temperature/K	109(13)
Crystal system	orthorhombic
Space group	$P2_12_12$
a/Å	28.4265(7)
b/Å	27.2114(9)
c/Å	10.4341(3)
α/°	90
β/°	90
γ/°	90
Volume/Å^3	8071.0(4)
Z	4
ρ_{calc}g/cm^3	1.311
μ/mm^{-1}	0.608
F(000)	3360.0
Crystal size/mm^3	0.334 × 0.296 × 0.227
Radiation	MoKα (λ = 0.71073)
2Θ range for data collection/°	4.714 to 58.862
Index ranges	-38 ≤ h ≤ 35, -32 ≤ k ≤ 36, -14 ≤ l ≤ 14
Reflections collected	75037
Independent reflections	19396 [R_{int} = 0.0724, R_{sigma} = 0.0842]
Data/restraints/parameters	19396/109/1004
Goodness-of-fit on F^2	1.099
Final R indexes [I>=2σ (I)]	R_1 = 0.0633, wR_2 = 0.1235
Final R indexes [all data]	R_1 = 0.0805, wR_2 = 0.1310
Largest diff. peak/hole / e Å^{-3}	1.22/-0.56
Flack parameter	0.011(5)

CPL Brightness

Table S2. Photophysical Parameters and B_{CPL} of (R-H_8-Binol)$_3$LnNa$_3$ (Ln = Sm, Tb, Dy)

(H_8-Binol)$_3$LnNa$_3$	ε/$M^{-1}cm^{-1}$ (λ_{abs}/nm)	Φ	Transition	$\lvert g_{lum}\rvert$ (λ/nm)	β	B_{CPL}/ $M^{-1}cm^{-1}$
Ln = Sm	27000 (310)	0.04	$^4G_{5/2} \longrightarrow {}^6H_{5/2}$	0.31 (576)	0.08	13.4
			$^4G_{5/2} \longrightarrow {}^6H_{7/2}$	0.44 (603)	0.16	38.0
			$^4G_{5/2} \longrightarrow {}^6H_{9/2}$	0.07 (653)	0.48	18.1
Ln = Tb	27000 (310)	0.27	$^5D_4 \longrightarrow {}^7F_6$	0.21 (490)	0.13	99.5
			$^5D_4 \longrightarrow {}^7F_5$	0.32 (542)	0.67	782
			$^5D_4 \longrightarrow {}^7F_4$	0.22 (597)	0.07	56.1
			$^5D_4 \longrightarrow {}^7F_3$	0.25 (628)	0.08	72.9
Ln = Dy	27000 (310)	0.17	$^4F_{9/2} \longrightarrow {}^6H_{15/2}$	0.18 (477)	0.06	24.8
			$^4F_{9/2} \longrightarrow {}^6H_{13/2}$	0.03 (594)	0.82	56.5
			$^4F_{9/2} \longrightarrow {}^6H_{11/2}$	0.32 (668)	0.05	36.7
			$^4F_{9/2} \longrightarrow {}^6H_{9/2}$	0.33 (756)	0.04	30.3

B_{CPL} values are calculated according to the equation: $B_{CPL} = ½\ \beta \times \varepsilon_\lambda \times \Phi \times g_{lum}$ (unit: $M^{-1}cm^{-1}$).[3]

Table S3. Photophysical Parameters and B_{CPL} of (bmpbp)Ln(OTf)$_3$ (Ln = Sm, Eu Tb, Dy)[4]

(bmpbp)Ln(OTf)$_3$	ε/$M^{-1}cm^{-1}$ (λ_{abs}/nm)	Φ	Transition	$\lvert g_{lum}\rvert$ (λ/nm)	β	B_{CPL}/ $M^{-1}cm^{-1}$
Ln = Sm	24000 (305)	0.0047	$^4G_{5/2} \longrightarrow {}^6H_{5/2}$	0.25 (577)	0.08	1.13
			$^4G_{5/2} \longrightarrow {}^6H_{7/2}$	0.16 (598)	0.44	3.97
			$^4G_{5/2} \longrightarrow {}^6H_{9/2}$	0.03 (646)	0.26	0.440
Ln = Eu	24000 (305)	0.16	$^5D_0 \longrightarrow {}^7F_1$	0.06 (592)	0.14	16.1
			$^5D_0 \longrightarrow {}^7F_2$	0.05 (620)	0.31	29.8
			$^5D_0 \longrightarrow {}^7F_3$	0.22 (653)	0.04	16.9
			$^5D_0 \longrightarrow {}^7F_4$	0.03 (703)	0.38	21.9
Ln = Tb	24000 (305)	0.32	$^5D_4 \longrightarrow {}^7F_6$	0.05 (492)	0.22	42.2
			$^5D_4 \longrightarrow {}^7F_5$	0.19 (543)	0.42	306
			$^5D_4 \longrightarrow {}^7F_4$	0.05 (587)	0.20	38.4
			$^5D_4 \longrightarrow {}^7F_3$	0.21 (625)	0.09	72.6
Ln = Dy	24000 (305)	0.0033	$^4F_{9/2} \longrightarrow {}^6H_{15/2}$	0.03 (485)	0.40	0.475
			$^4F_{9/2} \longrightarrow {}^6H_{13/2}$	0.03 (571)	0.42	0.499
			$^4F_{9/2} \longrightarrow {}^6H_{11/2}$	0.26 (673)	0.03	0.309

B_{CPL} values are calculated according to the equation: $B_{CPL} = ½\ \beta \times \varepsilon_\lambda \times \Phi \times g_{lum}$ (unit: $M^{-1}cm^{-1}$).[3]

Table S4. Photophysical Parameters and B_{CPL} of (tpdac)Ln(OTf)$_3$ (Ln = Sm, Eu, Tb, Dy)[5]

(tpdac)Ln(OTf)$_3$	ε/$M^{-1}cm^{-1}$ (λ_{abs}/nm)	Φ	Transition	$\lvert g_{lum}\rvert$ (λ/nm)	β	B_{CPL}/ $M^{-1}cm^{-1}$
Ln = Sm	3300 (260)	0.0017	$^4G_{5/2} \longrightarrow {}^6H_{5/2}$	0.13 (563)	0.12	0.0438
			$^4G_{5/2} \longrightarrow {}^6H_{7/2}$	0.06 (597)	0.54	0.0909
			$^4G_{5/2} \longrightarrow {}^6H_{9/2}$	0.05 (643)	0.34	0.0477
Ln = Eu	3600 (260)	0.018	$^5D_0 \longrightarrow {}^7F_1$	0.06 (591)	0.17	0.330
			$^5D_0 \longrightarrow {}^7F_2$	0.06 (615)	0.31	0.603

			$^5D_0 \longrightarrow {}^7F_3$	0.09 (648)	0.05	0.146
			$^5D_0 \longrightarrow {}^7F_4$	0.07 (690)	0.46	1.04
Ln = Tb	5600 (260)	0.28	$^5D_4 \longrightarrow {}^7F_6$	0.02 (489)	0.22	3.45
			$^5D_4 \longrightarrow {}^7F_5$	0.17 (542)	0.44	58.6
			$^5D_4 \longrightarrow {}^7F_4$	0.07 (582)	0.21	11.5
			$^5D_4 \longrightarrow {}^7F_3$	0.10 (622)	0.10	7.84
Ln = Dy	5600 (260)	0.0043	$^4F_{9/2} \longrightarrow {}^6H_{15/2}$	0.05 (479)	0.44	0.265
			$^4F_{9/2} \longrightarrow {}^6H_{13/2}$	0.02 (575)	0.51	0.123
			$^4F_{9/2} \longrightarrow {}^6H_{11/2}$	0.15 (665)	0.05	0.0903

B_{CPL} values are calculated according to the equation: $B_{CPL} = ½ \beta \times \varepsilon_\lambda \times \Phi \times g_{lum}$ (unit: $M^{-1}cm^{-1}$).[3]

Table S5. Photophysical Parameters and B_{CPL} of $[LnBnMeH22IAM]^+$ (Ln = Sm, Dy)[6]

$[LnBnMeH22IAM]^+$	$\varepsilon/M^{-1}cm^{-1}$ (λ_{abs}/nm)	Φ	Transition	$\lvert g_{lum}\rvert$ (λ/nm)	β	B_{CPL}/ $M^{-1}cm^{-1}$
Ln = Sm	25000 (346)	0.008	$^4G_{5/2} \longrightarrow {}^6H_{5/2}$	0.027 (565)	0.10	0.270
			$^4G_{5/2} \longrightarrow {}^6H_{7/2}$	0.028 (597)	0.40	1.12
Ln = Dy	25000 (346)	0.013	$^4F_{9/2} \longrightarrow {}^6H_{11/2}$	0.013 (669)	0.09	0.190

B_{CPL} values are calculated according to the equation: $B_{CPL} = ½ \beta \times \varepsilon_\lambda \times \Phi \times g_{lum}$ (unit: $M^{-1}cm^{-1}$).[3]

Note: The other papers cited in the manuscript lack information for doing circularly polarized luminescence brightness calculations, therefore, we only included several examples we could get.

Reference

(1). A. Korostylev, V. I. Tararov, C. Fischer, A. Monsees and A. Börner, *J. Org. Chem*., 2004, **69**, 3220–3221.

(2). a) A. de Bettencourt-Dias, P. S. Baber, S. Viswanathan, D. T. de Lill, A. Rollet, G. Ling and S. Altun, *Inorg. Chem*., 2010, **49**, 8848–8861. b) A. de Bettencourt-Dias, P. S. Barber and S. Bauer, *J. Am. Chem. Soc.*, 2012, **134**, 6987–6994. c) A. de Bettencourt-Dias, S. Bauer, S. Viswanathan, B. C. Maull and A. M. Ako, *Dalton Trans.*, 2012, **41**, 11212–11218.

(3). L. Arrico, L. Di Bari and F. Zinna, *Chem. Eur. J*., 2020, DOI:10.1002/chem.202002791.

(4). D. Schnable, K. Freedman, K. M. Ayers, N. D. Schley, M. Kol and G. Ung, *Inorg. Chem*., 2020, **59**, 8498–8504.

(5). K. Ayers, N. D. Schley and G. Ung, *Inorg. Chem*., 2020, **59**, 7657–7665.

(6). S. Petoud, G. Muller, E. G. Moore, J. Xu, J. Sokolnicki, J. P. Riehl, U. N. Le, S. M. Cohen and K. N. Raymond, *J. Am. Chem. Soc*., 2007, **129**, 77–83.